2-[^{11}C]Thymidine Positron Emission Tomography Reproducibility in Humans

Paula Wells,[1] Roger N. Gunn,[2] Colin Steel,[3] Alex S. Ranicar,[3] Frank Brady,[3] Safiye Osman,[3] Terry Jones,[2] and Pat Price[1]

Abstract

Purpose: To evaluate the reproducibility of 2-[^{11}C]thymidine positron emission tomography (PET) scanning in patients with advanced intra-abdominal malignancies.

Patients and Methods: The reproducibility of 2-[^{11}C]thymidine PET was studied by comparing interpatient and intrapatient variability (coefficient of variability, COV) of both blood and tissue data. Arterial plasma metabolite levels were measured using on-line sampling and high-pressure liquid chromatography. 2-[^{11}C]Thymidine retention in tissue was measured as the standardized uptake value at the end of the scan (SUV_{end}), the area under the time-activity curve ($AUC_{0\text{-}1\ hour}$), and the fractional retention of thymidine (FRT). A group of seven patients were scanned 1 week apart with no intervening anticancer therapy.

Results: There was interpatient variability in the levels of 2-[^{11}C]thymidine and its main metabolite, $^{11}CO_2$, in plasma. Variability in 2-[^{11}C]thymidine PET data was greater between (COV: SUV_{end} = 38%, $AUC_{0\text{-}1\ hour}$ = 32%, FRT = 47%) than within (COV: SUV_{end} = 8%, $AUC_{0\text{-}1\ hour}$ = 2%, FRT = 9%) patients. There was a borderline significant difference between the paired tumor data for SUV_{end} ($P = 0.041$), but not for $AUC_{0\text{-}1\ hour}$ ($P = 0.81$) or FRT ($P = 0.90$). There was a good correlation between paired data for SUV_{end} ($r = 0.98$), $AUC_{0\text{-}1\ hour}$ ($r = 0.99$), and FRT ($r = 0.95$).

Conclusions: This is the first report showing that 2-[^{11}C]thymidine PET scanning is reproducible in humans. Repeat scanning of tumor proliferation using 2-[^{11}C]thymidine PET is feasible to perform in human intra-abdominal malignancies and should aid the future rapid assessment of antiproliferative tumor agents.

Clinical drug development would be assisted greatly by the development of surrogate end points that could provide early and objective evidence of clinical activity. It is an issue that is becoming increasingly important as anticancer drug development diversifies away from a conventional antiproliferative approach to tumor-targeted strategies that focus on differing aspects of tumor versus normal tissue biology, such as increased angiogenesis and changes in signal transduction. The lack of conventional side effects associated with these new approaches to cancer treatment provides the rationale behind research into surrogate end points that could be used to optimize clinical dose and schedule finding studies. Noninvasive imaging is one approach that is currently under investigation as a method to test the "proof of principle" of the activity of new anticancer agents undergoing clinical evaluation (1–3).

The development of positron emission tomography (PET) to measure the pharmacodynamic effects of cancer treatment has focused on the most widely studied tracer, [^{18}F]fluorodeoxyglucose (4–7). [^{18}F]Fluorodeoxyglucose is taken up into tumor cells by Glut-1 receptors, and uptake is related to cell number (8–10). The potential of PET for predicting tumor response in the phase I setting was shown in a study of the tyrosine kinase inhibitor imatinib (STI571) in metastatic gastrointestinal tumors (11). It is likely, however, that a more specific tracer would provide direct physiologic information about tumor function, whereas reducing the confounding influence of fluorodeoxyglucose uptake into tumor normal cell infiltrates (5, 12). 2-[^{11}C]Thymidine PET is being assessed in man as a specific measure of tumor proliferation. Uptake of 2-[^{11}C]thymidine is related to DNA synthesis (13) and, in comparison with [^{18}F]fluorodeoxyglucose, it has been shown to be a more sensitive discriminator of early clinical response in small cell lung cancer and sarcoma (14). Our own studies in advanced human intra-abdominal malignancies have recently shown that 2-[^{11}C]thymidine PET data correlate with *ex vivo* measurements of the Ki-67 index (15), and that the tracer can measure thymidylate synthase inhibition (16).

2-[^{11}C]Thymidine PET will only be useful as a surrogate measure of clinical response if it can be shown to be a reproducible technique. Unfortunately, there are no published studies assessing intrapatient variability of 2-[^{11}C]thymidine

Authors' Affiliations: [1]Department of Cancer Medicine, [2]Medical Research Council Cyclotron Unit, and [3]Hammersmith Imanet, Imperial College London, Hammersmith Hospital, London, United Kingdom

Received 9/6/04; revised 2/21/05; accepted 3/30/05.

Grant support: Medical Research Council of the United Kingdom, Cancer Research UK grants C153/A1797 and C153/A1802, and National Cancer Institute grant ROI CA83028.

The costs of publication of this article were defrayed in part by the payment of page charges. This article must therefore be hereby marked *advertisement* in accordance with 18 U.S.C. Section 1734 solely to indicate this fact.

Requests for reprints: Pat Price, Manchester Molecular Imaging Center, University of Manchester, Wolfson Building, 27 Palatine Road, Manchester M20 3LJ, United Kingdom. Phone: 44-161-446-8003; Fax: 44-161-446-8111; E-mail: pat.price@manchester.ac.uk.

PET. The reproducibility of PET metabolic measurements in malignant tumors has been shown using [^{18}F]fluorodeoxyglucose PET. In a study of 16 patients participating in phase I trials of novel antineoplastic compounds, repeat scans within 10 days with no intervening therapy yielded highly reproducible quantitative parameters of tumor glucose metabolism (17). Fluorodeoxyglucose, however, does not produce labeled metabolites that can interfere with the measurement of PET tracer uptake into tumor cells. Therefore, there is a need to show the reproducibility of readily metabolized tracers, such as 2-[^{11}C]thymidine. The aim of the work reported in this paper, therefore, was to examine the reproducibility of 2-[^{11}C]thymidine PET by performing serial scans on patients with advanced intra-abdominal cancers.

Patients and Methods

Patients. The PET study was approved by the ethical committee of the Imperial College School of Medicine, Hammersmith Hospital, London, United Kingdom. Permission to administer the radioactive tracers was obtained from the Administration of Radioactive Substances Advisory Committee of the United Kingdom. Forty-five patients, with ages from 29 to 86 years (mean 52 years), with advanced intra-abdominal malignancies were enrolled. All gave their written informed consent. The study comprised treatment-naïve patients with a performance status ≤1 (i.e., patients asymptomatic or symptomatic but fully ambulatory). To minimize intrapatient variability in hepatic and portal venous flow and the effect of circadian variations in metabolism, patients fasted for a minimum of 4 hours and were scanned at a similar time of day (18).

Patient imaging. Imaging was done on an ECAT 931-08/12 scanner (CTI/Siemens, Knoxville, TN) at the Hammersmith Hospital after insertion in different limbs of arterial and i.v. cannulae for blood sampling and injection of radiotracer, respectively. Patient position was defined by X-ray simulation of the area of interest following localization of the tumor position from a recent computed tomography scan. A ^{68}Ge phantom was used to calibrate the PET data with radioactivity measured in a well counter. 2-[^{11}C]Thymidine was produced as described elsewhere (19) and administered i.v. as a bolus over 30 seconds, 30 seconds after the start of scanning. An on-line measuring system was used to record the radioactivity of arterial blood samples at 1-second intervals. Discrete blood samples were also taken to calibrate the radioactive counts, and the relative amounts of parent and metabolite compounds in the plasma were measured using high-performance liquid chromatography (20). A time course for the release of $^{11}CO_2$ in expired air was also obtained using nasal sampling (21). Metabolite data from blood samples and exhaled $^{11}CO_2$ were used to correct the total plasma input function for the contribution from labeled metabolites and to produce parent thymidine, intermediate metabolite (thymine, dihydrothymine, β-aminobutyric acid), and CO_2 input functions (21, 22).

Positron emission tomography image analysis. Sinogram data were reconstructed into tomographic images using filtered back projection after transfer to a Sun SPARC Workstation (Sun Microsystem, Mountain View, CA). Voxel dimensions were 2.1 × 2.1 × 6.4 mm and the full-width half-maximum values at the center of the field of view were 8.4, 8.3, and 6.6 mm, respectively. Inspection of a recent computed tomography scan was used to assist the delineation of tumor and normal tissue regions. Regions of interest were drawn by hand, guided by diagnostic imaging, and defined using Analyze image analysis software (Biomedical Imaging Resource, Mayo Foundation) on integral images rather than individual time frames. All tumors >4 cm^2 contained areas of central necrosis that were excluded from the region of interest. Regions of interest were variable for tumors, but of similar size for normal tissues. Partial volume effects were minimized by using a minimum of five contiguous planes but not sampling the first and last two planes of an organ of interest, and by avoiding organ edges. Application of each region of interest to the corresponding dynamic image data yielded a time-activity curve.

Quantification of tissue tracer uptake. The tumor and plasma 2-[^{11}C]thymidine time-activity curves were used to calculate three parameters. 2-[^{11}C]Thymidine data were normalized to account for patient body weight and injected dose to give the standardized uptake curve. The parameter SUV_{end} (standardized uptake value at the end of the scan) in g/mL was calculated as the average value between 3,000 and 3,600 seconds. The parameter $AUC_{0\text{-}1\ hour}$ (area under the time-activity curve) in g-h/mL was calculated as the integral of the standardized uptake curve from injection to the end of the scan (3,600 seconds). The fractional retention of thymidine (FRT) parameter was calculated by tracer kinetic modeling using spectral analysis, which calculates the tumor impulse response function (IRF) from the metabolite corrected plasma input function and the corresponding tumor time-activity curve (23). Values for IRF were obtained for the delivery ($IRF_{1\ minute}$) and the retention ($IRF_{60\ minutes}$) of the tracer in tissue and the fractional retention at 1 hour (FRT) was calculated as $IRF_{60\ minutes}/IRF_{1\ minute}$. FRT values can range from 0 to 1 corresponding with 0% to 100% of the delivered tracer being retained in a tissue at 60 minutes.

Statistical analyses. The variability of the blood and tissue data was expressed as a coefficient of variability (COV; SD / mean × 100, expressed as a percentage). Intrapatient reproducibility was investigated

Table 1. Variability in plasma tracer and metabolite levels

Time (min)	2-[^{11}C]Thymidine		$^{11}CO_2$		
	Mean ± SD* (%)	COV† (%)	Mean ± SD* (%)	COV† (%)	COV‡ (%)
1.50	90.1 ± 3.4	4	2.7 ± 5.0	186	37§
2.50	62.8 ± 9.0	14	24.7 ± 14.2	57	11
3.50	32.5 ± 9.2	28	46.2 ± 12.7	27	2
5.25	13.9 ± 5.1	37	56.9 ± 13.0	23	1
7.75	7.8 ± 2.5	32	63.1 ± 13.7	22	2
15.25	5.1 ± 2.2	44	67.7 ± 13.7	20	2

*Values are percentages of the total plasma activity and are the mean and SD of data from 39 patients.
†Interpatient COV.
‡Intrapatient COV was determined in four patients by taking three repeat estimates of plasma $^{11}CO_2$ during the same scanning session. The values are the mean COV for the four patients.
§Data for two patients only; for the remaining two patients, counts were too low to obtain reliable repeat estimates.

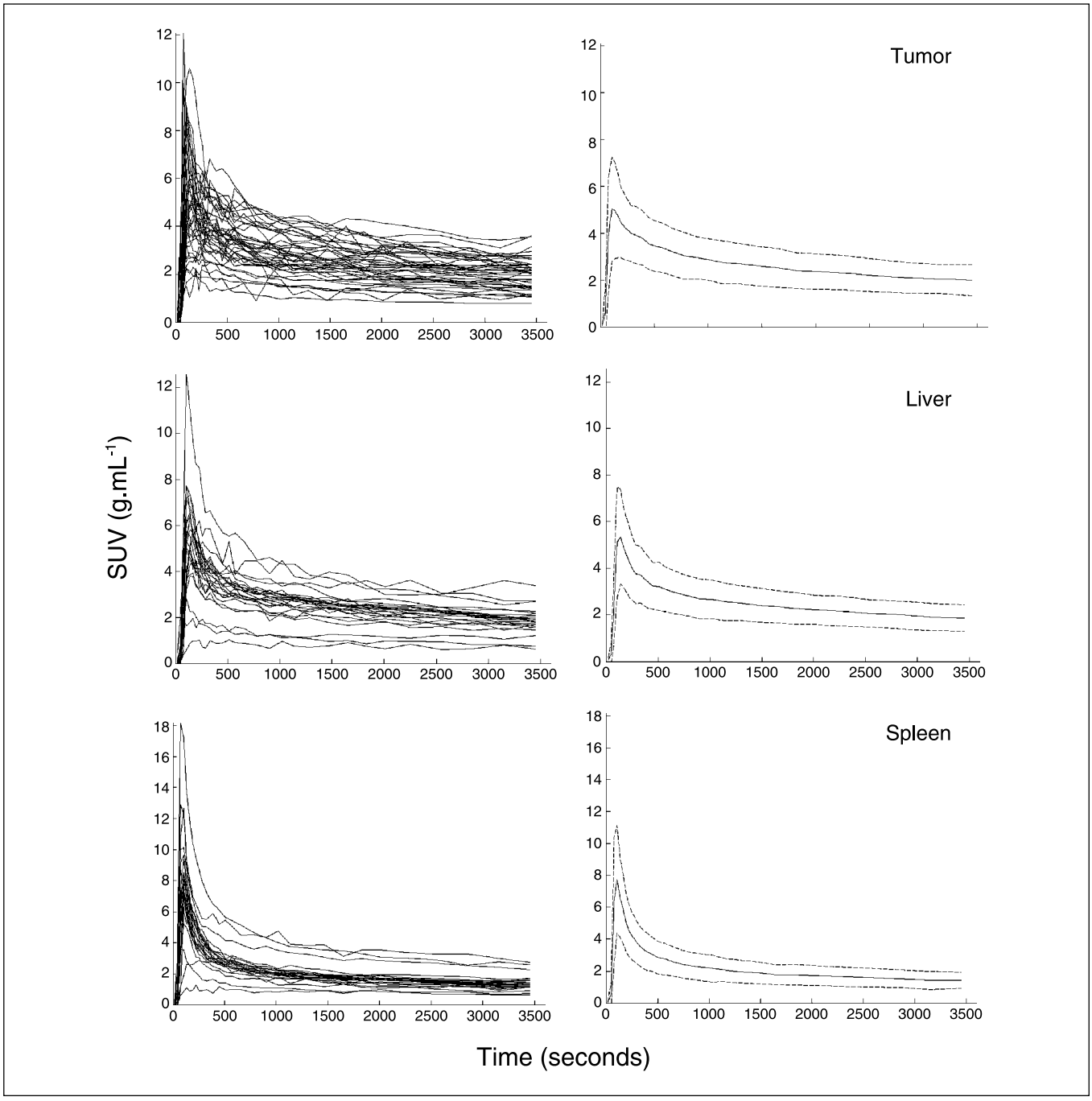

Fig. 1. Interpatient variability in 2-[^{11}C]thymidine PET. Tumor (n = 45 patients), liver (n = 26 patients), and spleen (n = 22 patients) time-activity curves from patients with advanced intra-abdominal malignancies (*left*). SUV is the tissue activity corrected for differences in body weight and injected radiotracer dose. The mean curve with ±1 SD is also shown (*right*).

using a paired t test (two tailed), Pearson's correlation coefficient, and the intraclass correlation coefficient. A probability of $P = 0.05$ was used throughout to indicate a statistically significant result.

Results

Variability in plasma tracer and metabolite estimations. Forty-one of the 45 enrolled patients with advanced intra-abdominal malignancies (14 females and 27 males) were assessed for variability in blood tracer and metabolite estimations. Arterial data were not collected in the remaining four patients because of problems with the insertion of arterial cannulae. Due to the limitations of the sensitivity of the detection system for high-performance liquid chromatography analysis and the rapid clearance of 2-[^{11}C]thymidine, the threshold for high-performance liquid chromatography analysis was limited to 15 minutes from the start of scanning. In 2 of the 41 patients the plasma, 2-[^{11}C]thymidine levels derived by high-performance

Table 2. Patient characteristics and repeat tumor PET 2-[^{11}C]thymidine parameter data

Pt	Primary site	Imaged site	Age (y)	PS	Injected activity		SUV_{end}		$AUC_{0\text{-}1\ hour}$		FRT	
					1st	2nd	1st	2nd	1st	2nd	1st	2nd
1	Cholangiocarcinoma	Liver	39	0	323	135	2.61	2.15	205	205	0.287	0.304
2	Colorectal	Liver	61	1	383	274	1.37	1.56	131	130	0.189	0.152
3	Stomach	Lung	71	1	375	272	1.05	1.10	85	84	0.390	0.372
4	Colorectal	Liver	60	1	557	534	2.27	2.00	100	110	0.204	0.193
5	Colorectal	Liver	76	1	388	265	3.70	3.43	120	120	0.372	—
6	Pancreas	Pancreas	68	0	481	373	1.45	1.23	167	158	0.204	0.193
7	Pancreas	Pancreas	53	0	413	475	1.49	1.55	247	250	0.149	0.195

NOTE: Injected activity is expressed in MBq. SUV_{end} in g/mL is calculated as the average value between 3,000 and 3,600 seconds. $AUC_{0\text{-}1\ hour}$ is expressed in g-h/mL. A second FRT measurement was not obtained in one patient because of an inadequate input function.
Abbreviations: Pt, patient number; PS, WHO performance status.

liquid chromatography were too low for accurate quantification and these patients were removed from the analysis. Table 1 summarizes the data for the remaining 39 patients. 2-[^{11}C]Thymidine cleared rapidly from plasma and was degraded via its main radioactive metabolites to $^{11}CO_2$, the final labeled species. Three minutes after injection, $^{11}CO_2$ was the main labeled species in plasma. The 11-fold rise in the COV with time shows that the interpatient variability in the fraction of 2-[^{11}C]thymidine in plasma increased with time following the start of scanning. Although the interpatient variability in plasma $^{11}CO_2$ levels decreased with time, the COV remained at 20% 15 minutes following the start of scanning. In four patients, variability in the estimation of plasma $^{11}CO_2$ was measured by obtaining triplicate samples during a single scanning session. This intrapatient variability in the estimation of plasma $^{11}CO_2$ was around 10-fold lower than that seen between patients. By 3.5 to 15.25 minutes following the start of scanning, intrapatient COVs were only 1% to 2%.

Variability in tumor tracer pharmacokinetics. Tissue tracer pharmacokinetics were studied in 45 treatment-naïve patients with advanced intra-abdominal tumors (17 females and 28 males). The injected tracer data ranged from 80 to 689 MBq (mean 375 MBq) for dose, 5,400 to 63,100 MBq/μmol (mean 16,300 MBq/μmol) for specific activity and 97.4% to 100% (mean 99.4%) for radiochemical purity. The tumor time-activity curves were similar in shape for all the patients (Fig. 1). The uptake of tracer into tissue was rapid, reaching a maximum within 1 to 2 minutes, and was followed by a slower washout period. To assess intra-patient variability, repeat scans were done on a subset of seven patients. These patients were selected on the basis of being willing and able to undergo a second scan. The patient characteristics and data for these seven patients are given in Table 2. There was a borderline significant difference between the paired tumor data for SUV_{end} ($P = 0.041$), but not for $AUC_{0\text{-}1\ hour}$ ($P = 0.81$) or FRT ($P = 0.90$). Table 3 summarizes the PET parameter data. There was more variability

Table 3. A comparison of interpatient and intrapatient variability in PET parameters of 2-[^{11}C]thymidine retention in different tissues

Parameter	Tissue (*n*)	Mean ± SD	COV (%)	
			Interpatient	Intrapatient
SUV_{end}	Tumor (45)	2.00 ± 0.80	38	8*
	Liver (26)	1.90 ± 0.85	45	13†
	Spleen (22)	1.40 ± 0.17	40	13†
$AUC_{0\text{-}1\ hour}$	Tumor (45)	155 ± 49	32	2*
	Liver (26)	157 ± 33	21	8†
	Spleen (22)	119 ± 5	4	5†
FRT	Tumor (36)	0.30 ± 0.14	47	9†
	Liver (26)	0.23 ± 0.08	35	4‡
	Spleen (22)	0.15 ± 0.03	20	24§

NOTE: *n*, total number of patients scanned. Data are missing because of an inadequate volume of normal tissue within the PET image or because an input function could not be obtained (FRT).
*Seven patients were scanned for the assessment of intrapatient COV.
† $n = 6$.
‡ $n = 4$.
§ $n = 5$.

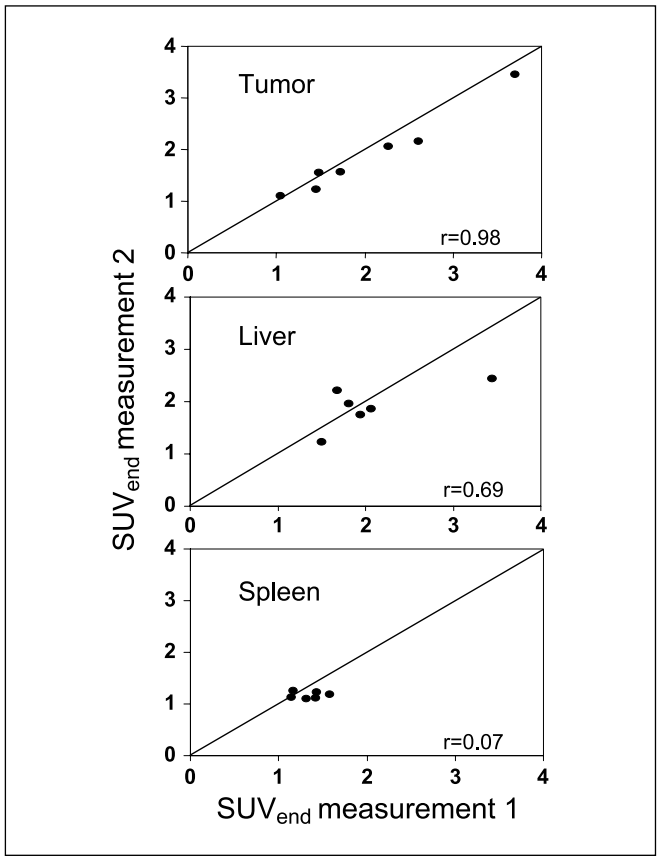

Fig. 2. Intrapatient variability in 2-[^{11}C]thymidine PET. SUV$_{end}$ is calculated from the tissue activity curves illustrated in Fig. 1 at the end of the scanning period (average value between 3,000 and 3,600 seconds). Patients with advanced intra-abdominal cancer were scanned twice with an interval of 1 week. The lines of identity are shown.

in the data between than within patients. There was a good correlation between the paired data for SUV$_{end}$ (r = 0.98), AUC$_{0\text{-}1\ hour}$ (r = 0.99), and FRT (r = 0.95). The intraclass correlation coefficients were 0.96, 0.99, and 0.95, respectively. Figures 2–4 illustrate the correlations between the test-retest data.

Variability in normal tissue tracer pharmacokinetics. Normal tissue time-activity curves were generated for a subset of the patients for whom an adequate volume of normal tissue was available in the PET image. The liver curves were similar to tumor, but the spleen curves showed a rapid influx of tracer that was of greater magnitude than for tumor (Fig. 1). A subsequent rapid decrease resulted in low tracer retention in the spleen. Interpatient variability was generally lower in liver and spleen than in tumor (Table 3), which probably reflects greater tissue homogeneity. Tracer retention measured as FRT was highest in tumor and lowest in spleen.

Discussion

This study has shown that PET-derived parameters of thymidine tracer incorporation are reproducible in patients with advanced intra-abdominal malignancies. The analysis of PET images following administration of the readily metabolized [^{11}C]thymidine tracer is facilitated by measuring the levels of metabolites in blood and tissue, and applying a suitable model (24, 25). Although pooled population input functions would be easier to use on a routine clinical basis, there was interpatient variability in the levels of CO_2 in plasma. Therefore, the results reported here show that for the calculation of FRT using [^{11}C]thymidine, individual plasma input functions should be used and arterial blood sampling is required for all patients. This finding mirrors the results from other groups working on [^{11}C]thymidine PET in head and neck (26), and predominantly lung (27), cancers. For example, the Shields et al. (27) study showed that 2.9 minutes following injection, 50% of the total radioactivity in blood was due to labeled thymidine. The interpatient COV was 21%. These values are similar to those reported here, where at 2.5 minutes 63% of blood radioactivity was due to thymidine and the interpatient COV was 14%.

There is no published literature describing the scanning variability of 2-[^{11}C]thymidine PET in humans. [^{18}F]fluorodeoxyglucose PET has been shown to be reproducible in normal brain tissue (28) and malignant tumors (17, 29). Fluorodeoxyglucose, however, is not a metabolized PET tracer, and the work here is, to our knowledge, the first report showing the reproducibility of PET in humans following injection of the

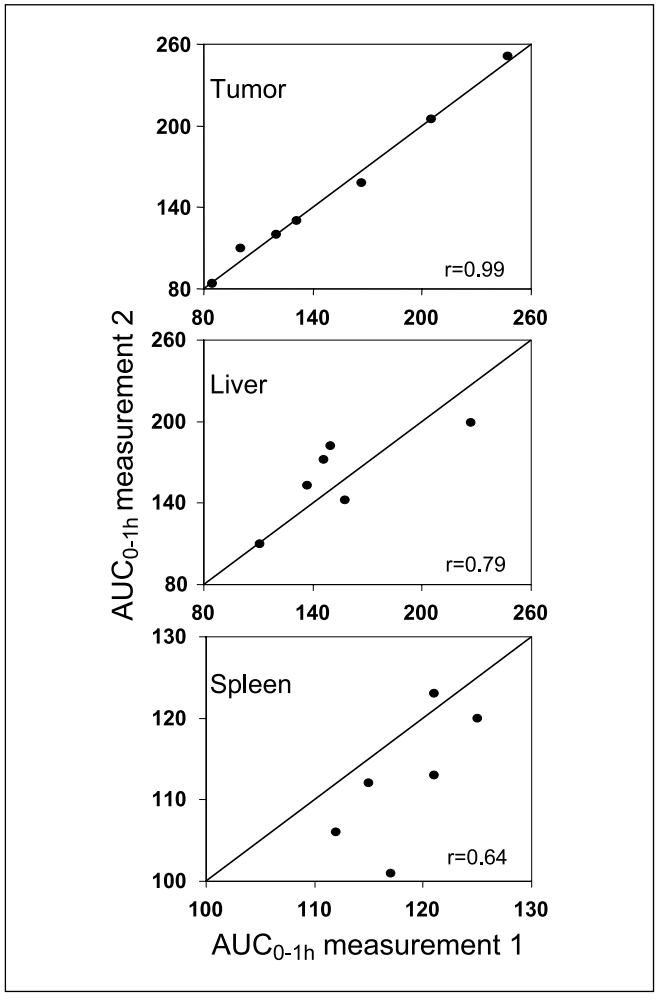

Fig. 3. Intrapatient variability in 2-[^{11}C]thymidine PET. The AUC$_{0\text{-}1\ hour}$ parameter is calculated from the tissue activity curves illustrated in Fig. 1 up to the end of the scanning period (3,600 seconds). Patients with advanced intra-abdominal cancer were scanned twice with an interval of 1 week. The lines of identity are shown.

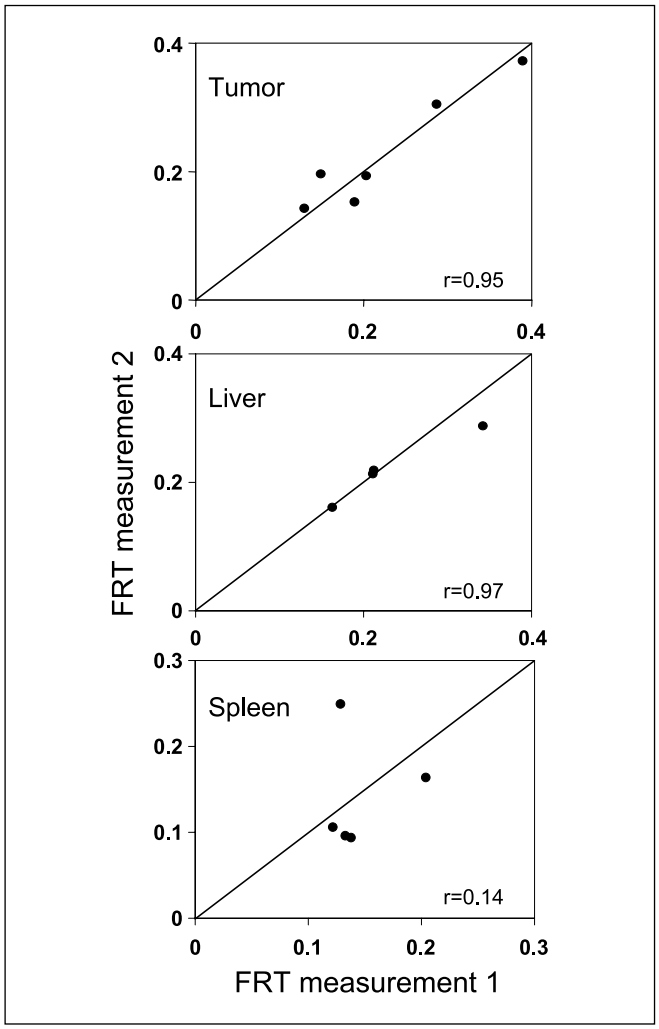

Fig. 4. Intra-patient variability in 2-[^{11}C]thymidine PET. The FRT parameter is calculated, using spectral analysis, from the tissue activity curves illustrated in Fig. 1. Patients with advanced intra-abdominal cancer were scanned twice with an interval of 1 week. The lines of identity are shown.

metabolized radiotracer 2-[^{11}C]thymidine. The interpatient variability in tracer retention was expected given the heterogeneous patient population that comprised both primary and metastatic disease, and lesions that arose from a variety of different organs. In addition, there is considerable intratumor and intertumor variability in proliferation even between tumors of the same etiology (30). As PET data are commonly presented as SUV and AUC, the parameters are described within this paper. Both interpatient and intrapatient variability were less for AUC than SUV. This observation probably relates in part to differences in the contribution of statistical image noise, because the AUC includes a greater fraction of the time course of tissue uptake curves and, therefore, includes more image counts. However, SUV and AUC are not based on kinetic models; a large part of the measured radioactivity can be attributed to the presence of labeled metabolites and unincorporated thymidine and their meaning is difficult to interpret. In comparison with SUV and AUC, FRT lessens the bias caused by labeled metabolites and unincorporated thymidine. We have previously shown that the FRT correlates with *ex vivo* measurements of tumor proliferation using the Ki-67 index (15). In this publication we have extended that finding by showing that measurements of FRT in human intra-abdominal cancers are reproducible. Interpatient variability was at least 5-fold higher than intrapatient variability, with COVs of 47% and 9%, respectively. Therefore, these data support the use of FRT for pharmacodynamic studies of novel antiproliferative agents.

It is of interest to note that similar patterns of tracer uptake and retention were seen for the tumor and normal tissues studied (Fig. 1). The peak tracer delivery and the washout phase are influenced by labeled tracer/metabolite retention in tissues. Variability in the curves between and within tissues reflects differences in pathology, physiology, function, and the retention of labeled tracer/metabolites. In the liver, it is likely that the main factors that influence tracer kinetics are the delivery and metabolism of the tracer. Work in animals has shown that the liver is an important site of 2-[^{11}C]thymidine metabolism (31, 32), and that most of the measured radioactivity can be attributed to labeled metabolites. Despite expiration of large volumes of gaseous metabolites, large amounts of $^{11}CO_2$ can remain and contaminate blood and tissue data (24). Although intrapatient variability in FRT was highest in the spleen, this may be due to an outlier (Fig. 3). As expected, FRT was highest in tumor, the tissue with the highest level of proliferation.

In summary, this study has shown that 2-[^{11}C]thymidine PET is reproducible. The conclusion from this work is that repeat scanning using 2-[^{11}C]thymidine PET is feasible to perform in the phase I clinical trial setting and should aid the future rapid assessment of new antitumor agents.

References

1. Stroobants S, Goeminne J, Seegers M, et al. ^{18}FDG-Positron emission tomography for the early prediction of response in advanced soft tissue sarcoma treated with imatinib mesylate (Glivec). Eur J Cancer 2003; 39:2012–20.
2. Thomas JP, Arzoomanian RZ, Alberti D, et al. Phase I pharmacokinetic and pharmacodynamic study of recombinant human endostatin in patients with advanced solid tumors. J Clin Oncol 2003;21: 223–31.
3. Rowinsky EK, Hammond L, Siu L, et al. Dose-schedule-finding, pharmacokinetic, biologic, and functional imaging studies of OSI-774, a selective epidermal growth factor receptor (EGFR) tyrosine kinase inhibitor. Proc Am Soc Clin Oncol 2001;21: Abstract 5.
4. Young H, Baum R, Cremerius U, et al. Measurement of clinical and subclinical tumour response using [^{18}F]-fluorodeoxyglucose and positron emission tomography: review and 1999 EORTC recommendations. European Organization for Research and Treatment of Cancer (EORTC) PET Study Group. Eur J Cancer 1999;35:1773–82.
5. Price P. Changes in 18F-FDG uptake measured by PET as a pharacodynamic end-point in anticancer therapy. Br J Cancer 2000;83:281–3.
6. Brock CS, Meikle SR, Price P. Does fluorine-19 fluorodeoxyglucose metabolic imaging of tumours benefit oncology. Eur J Nucl Med 1997;24: 691–705.
7. Brock CS, Young H, O'Reilly SM, et al. Early evaluation of tumour metabolic response using [^{18}F]fluorodeoxyglucose and positron emission tomography: a pilot study following the phase II chemotherapy schedule for temozolomide in recurrent high-grade gliomas. Br J Cancer 2000;82:608–15.
8. Bos R, van Der Hoeven JJ, van Der Wall E, et al. Biologic correlates of (18)fluorodeoxyglucose uptake in human breast cancer measured by positron emission tomography. J Clin Oncol 2002;20:379–87.
9. Higashi K, Clavo AC, Wahl RL. Does FDG uptake measure proliferative activity of human cancer

cells? *In vitro* comparison with DNA flow cytometry and tritiated thymidine uptake. J Nucl Med 1993;34:414–9.

10. Smith TA. FDG uptake, tumour characteristics and response to therapy: a review. Nucl Med Commun 1998;19:97–105.

11. van Oosterom AT, Judson I, Verweij J, et al. Safety and efficacy of imatinib (STI571) in metastatic gastrointestinal stromal tumours: a phase I study. Lancet 2001;358:1421–3.

12. Kubota R, Yamada S, Kubota K, et al. Intratumoral distribution of fluorine-18-fluorodeoxyglucose *in vivo*: high accumulation in macrophages and granulation tissues studied by microautoradiography. J Nucl Med 1992;33:1972–80.

13. Vander Borght T, Lambotte L, Pauwels S, et al. Noninvasive measurement of liver regeneration with positron emission tomography and [2-^{11}C]thymidine. Gastroenterology 1991;101:794–9.

14. Shields AF, Mankoff DA, Link JM, et al. Carbon-11-thymidine and FDG to measure therapy response. J Nucl Med 1998;39:1757–62.

15. Wells P, Gunn RN, Alison M, et al. Assessment of proliferation *in vivo* using 2-[(11)C]thymidine positron emission tomography in advanced intra-abdominal malignancies. Cancer Res 2002;62:5698–702.

16. Wells P, Aboagye E, Gunn RN, et al. 2-[^{11}C]thymidine positron emission tomography as an indicator of thymidylate synthase inhibition in patients treated with AG337. J Natl Cancer Inst 2003;95:675–82.

17. Weber WA, Ziegler SI, Thodtmann R, Hanauske AR, Schwaiger M. Reproducibility of metabolic measurements in malignant tumors using FDG PET. J Nucl Med 1999;40:1771–7.

18. Torizuka T, Clavo AC, Wahl RL. Effect of hyperglycemia on *in vitro* tumor uptake of tritiated FDG, thymidine, L-methionine and L-leucine. J Nucl Med 1997;38:382–6.

19. Steel CJ, Brady F, Luthra SK, et al. An automated radiosynthesis of 2-[^{11}C]thymidine using anhydrous [^{11}C]urea derived from [^{11}C]phosgene. Appl Radiat Isot 1999;51:377–88.

20. Luthra SK. Labelling of compounds with positron-emitting isotopes for PET studies. In: Stewart MG, editor. Quantitative methods in neuroanatomy. New York: John Wiley and Sons, 1992.

21. Gunn RN, Ranicar A, Yap JT, et al. On-line measurement of exhaled [^{11}C]CO_2 during PET. J Nucl Med 2000;41:605–11.

22. Gunn RN, Yap JT, Wells P, et al. A general method to correct PET data for tissue metabolites using a dual-scan approach. J Nucl Med 2000;41:706–11.

23. Cunningham VJ, Jones T. Spectral analysis of dynamic PET studies. J Cereb Blood Flow Metab 1993;13:15–23.

24. Shields AF, Graham MM, Kozawa SM, et al. Contribution of labeled carbon dioxide to PET imaging of carbon-11-labeled compounds. J Nucl Med 1992;33:581–4.

25. Mankoff DA, Shields AF, Graham MM, et al. Kinetic analysis of 2-[carbon-11]thymidine PET imaging studies: compartmental model and mathematical analysis. J Nucl Med 1998;39:1043–55.

26. Goethals P, van Eijkeren M, Lodewyck W, Dams R. Measurement of [methyl-carbon-11]thymidine and its metabolites in head and neck tumors. J Nucl Med 1995;36:880–2.

27. Shields AF, Mankoff D, Graham MM, et al. Analysis of 2-carbon-11-thymidine blood metabolites in PET imaging. J Nucl Med 1996;37:290–6.

28. Maquet P, Dive D, Salmon E, von Frenckel R, Franck G. Reproducibility of cerebral glucose utilization measured by PET and the [^{18}F]-2-fluoro-2-deoxy-D-glucose method in resting, healthy human subjects. Eur J Nucl Med 1990;6:267–73.

29. Minn H, Zasadny KR, Quint LE, Wahl RL. Lung cancer: reproducibility of quantitative measurements for evaluating 2-[F-18]-fluoro-2-deoxy-D-glucose uptake at PET. Radiology 1995;196:167–73.

30. Palmqvist R, Oberg A, Bergstrom C, Rutegard JN, Zackrisson B, Stenling R. Systematic heterogeneity and prognostic significance of cell proliferation in colorectal cancer. Br J Cancer 1998;77:917–25.

31. Shields AF, Larson SM, Grunbaum Z, Graham MM. Short-term thymidine uptake in normal and neoplastic tissues: studies for PET. J Nucl Med 1984;25:759–64.

32. Shields AF, Lim K, Grierson J, Link J, Krohn KA. Utilization of labeled thymidine in DNA synthesis: studies for PET. J Nucl Med 1990;31:337–42.